2. MATERIALS DEVELOPMENT

A. Advanced Materials for Friction Brakes

Principal Investigator: P. J. Blau
Oak Ridge National Laboratory
P.O. Box 2008, Oak Ridge, TN 37831-6063
(865) 574-5377; fax: (865) 574-6918; e-mail:blaupj@ornl.gov

Chief Scientist: James J. Eberhardt
(202)586-9837; fax: (202)587-2476; e-mail: james.eberhardt@ee.doe.gov
Field Technical Manager: Philip S. Sklad
(865) 574-5069; fax: (865) 576-4963; e-mail: skladps@ornl.gov

---

Contractor: Oak Ridge National Laboratory
Contract No.: DE-AC05-00OR22725

Objectives

- Identify candidate materials for the next generation of high-performance, light-weight truck brakes; investigate their friction and wear characteristics; and provide data to support their introduction into the trucking industry.

Approach

- Design and build a subscale brake material testing apparatus to investigate the friction and frictional heating characteristics of advanced materials at speeds and contact pressures similar to those in full-sized brakes.
- Evaluate and understand the friction and thermal characteristics of candidate materials including titanium alloys, metal matrix composites, and ceramic matrix composites. Down-select the more promising materials, select appropriate linings to go with them, and focus on obtaining data to support their implementation on vehicles.
- Develop metrics for analyzing the dissipation of frictional energy in various braking material combinations, and apply that knowledge to the selection of brake material pairs.

Accomplishments

- Working the Dynamet Inc, obtained and evaluated the friction and frictional-heating characteristics of three experimental Ti-based, high-strength composites.
- Published a summary compilation of friction and thermo-physical properties data for all materials tested to-date.
- Working with Red Devil Brakes Company, obtained a set of full-sized, ceramic-coated titanium alloy truck brake rotors for dynamometer testing during FY 2006.

Future Direction

- Work with a leading truck brake system manufacturer to plan a testing program for ceramic-coated titanium brake rotors that were obtained during FY 2005.
- Continue to investigate novel methods to surface-engineer titanium-based rotor materials.
- Investigate carbon-based composite materials for possible use as rotors and/or pads.
- Identify lining materials that are frictionally compatible with advanced disc materials and develop a more fundamentals-based rationale for rotor/pad selection.

Introduction

Advanced aerodynamic designs and tires with lower rolling-resistance can improve the fuel efficiency of trucks. However, as these developments decrease the drag forces on trucks, the demands on braking systems increase. Brake engineering involves design, instrumentation and controls, and materials development. This project specifically addresses the latter. Brake materials must exhibit a balance of properties including frictional stability over a wide temperature range, appropriate thermal properties, dimensional stability, corrosion resistance to road deicers, and wear resistance. They must also be cost-competitive. Using non-traditional brake materials it may be possible to create lighter-weight braking systems that will enable improved fuel-efficiency without compromising vehicle safety and reliability.

This project concerns the selection and use of advanced structural materials and surface treatments that show potential as truck brake friction materials. Testing such new materials is made more cost-effective by using small specimens to screen the most promising candidates. To this end, a subscale brake tester (SSBT) was designed and built. It was instrumented to measure normal force, friction force, surface temperature and vibrations during braking. An attachable water spray system has enabled the effects of wet and dry braking to be studied. Analysis of SSBT results is supplemented by optical microscopy, scanning electron microscopy, and transmission electron microscopy of friction-induced surface films.

Prompted by stricter Department of Trans-portation regulations on stopping distances for trucks, air-disc brakes are beginning to replace drum brakes on new Class 8 trucks sold in the United States. Air disc brakes can achieve shorter stopping distances and are less likely to fade from overheating. With this trend in mind, the focus in this project has been on rotor materials for disc-brakes and the appropriate friction linings to mate with them.

Titanium-Based Candidate Rotor Materials

After evaluating the physical properties of candidate materials those with low-softening-points, brittle behavior, corrosion sensitivity, and environmentally unacceptable wear by-products were eliminated from consideration. A list of materials and the rationale for their selection were presented in the FY 2003 and FY 2004 Annual Reports.

During FY 2005, it was decided to focus on titanium (Ti)-based rotor materials, in metal matrix composites and as the structural material over which thermally-sprayed ceramic coatings were applied. Ti offers approximately 38% in weight savings compared to a comparably-sized cast iron rotor.

Titanium-based metal matrix composites (Ti-MMC) were selected and purchased from Dynamet, Inc. The Massachusetts firm has developed a proprietary cold and hot isostatic pressing (CHIP) process to manufacture Ti-based composites that can be produced with a variety of hard particles.

The surface-coated Ti samples were prepared by Red Devil Brakes Company, a Pennsylvania firm that developed a ceramic-based thermal spray process for coating Ti alloy brake rotors for high-performance racing applications. Coatings were typically about 1-2 mm thick.

Table 1 lists the Ti-alloy material combinations that were investigated. As in the past, pad materials were selected based on factors like the performance of similar linings against cast iron, recommendations from suppliers, and materials

Table 1. Ti-Based Friction Material Combinations.

Disc Specimen Material	Mating Material(s)
Titanium alloys (Ti-6Al-4V, and Ti-6Al-2Sn-4Zr-2Mo)	Jurid 539 disc brake lining
Ti-MMC with 10% TiC particles (CermeTi™ C-10) (Two thicknesses to evaluate thermal behavior)	Jurid 539 disc brake lining Performance FrictionCarbon-Metallic Pad (type 10)
Ti-MMC with 5% TiB2, balance: Ti-6Al-4V	Jurid 539 disc brake lining
Ti-MMC with 7.5% W, 7.5% TiC, balance: Ti-6Al-4V	Jurid 539 disc brake lining
Thermally-sprayed Titanium – Red Devil Brakes Co.	Metallic and semi-metallic pads materials supplied by Red Devil Brakes

whose thermo-physical properties made them likely partners. The pad materials may not necessarily be the optimum partners for the new rotor materials but they served as a means to compare friction characteristics in the SSBT relative to cast iron. For example, Jurid 539 is a semi-metallic disc brake lining material that is well known in the industry.

Experiments were conducted to characterize the effects of speed and contact pressure on the friction coefficient and frictional temperature rise for these Ti-MMC disc materials. Their thermo-physical properties were also measured at Oak Ridge National Laboratory (ORNL--H. Wang). Results are summarized in the following sections.

Studies of Titanium-Based Disc Materials

Table 2 lists the measured densities and thermophysical properties of the friction tested, candidate rotor materials. Symbols: kth is the thermal conductivity, □th is the thermal diffusivity, and Cp is the heat capacity.

Table 2. Property Data for Experimental Ti Materials Relative to that for Typical Gray Cast Iron.

Disc Material	Density (g/cm^3)	K_{th} (W/m-K)	□$_{th}$ (cm^2/s)	C_P (MJ/m^3-K)
Cast iron	7.2	42.-62.	-	-
Ti-6Al-4V	4.40	6.6	-	-
Ti -5TiB2	4.34	7.99	0.044	1.82
Ti-(7.5W, 7.5TiC)	4.68	6.57	0.028	2.36
Ti–10 TiC	4.37	6.89	0.029	2.41

Friction data were obtained on the materials listed in Table 1 under a variety of applied pressures and sliding velocities. A several step process is used to distill the 28,800 data values from each sliding test into a form that will reveal general trends in friction and temperature rise. For example, Figure 1 illustrates the effects of sliding speed on the friction of the Ti-based 5%TiB2 MMC slid against Jurid 539 pad material. Friction coefficients for typical brake linings against gray cast iron tend to fall within the range of 0.35 to 0.55, so the Ti-MMC data fall on the low end of conventional values. However, as pointed out earlier, use of an alternative lining material could likely improve this performance.

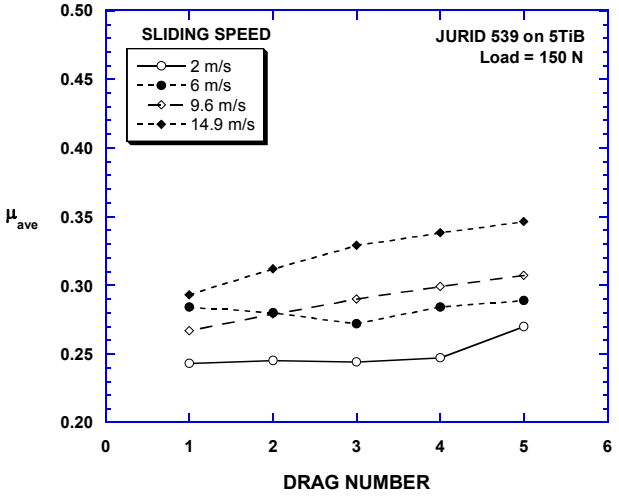

Figure 1. Effect of sliding speed on the friction of a TiB2 reinforced Ti-MMC (150N applied force).

Conversion of Friction into Heat

One convenient measure of the efficiency by which the frictional energy generated during braking is converted into heat is what is here called the 'thermal conversion parameter' (Qf) and is defined as follows:

$$Q_f = c\ (\ \Delta T / F\,x\ )$$

where ΔT is the temperature rise of the disc specimen surface during a constant speed drag, F is the average friction force, and x is the distance slid during the drag. The constant c is a function of the testing geometry and recognizes the fact that only the heating of the disc is considered, not the heating of the pad as well. Q_f can be thought of as the efficiency of a given rotor material in coverting frictional work (the product F x) into an observed surface temperature rise (ΔT). The higher Q_f, the more readily frictional work of braking translates into the heating of the disc surface.

Table 3 lists experimentally-measured values for several material combinations involving the Jurid 539 pad material and Ti-based materials. Cast iron, with its relatively high thermal conductivity, dissipates heat and has a lower Q_f, but the Ti-MMCs tend to run somewhat hotter. Adding thermally-conductive ceramic particles like TiB_2 tends to moderate that effect. Consequently, Ti-MMCs do not run quite as hot as the matrix alloy Ti-6Al-4V. Note that some of the previously tested ceramic composites, especially those with anisotropic microstructures, had Q_f values approaching 21. x 10^{-3} ^{o}C/N-m. Higher frictional heating behavior is acceptable as long as the high temperature strength and resistance to thermal distortion are adequate, but it also suggests that the use of materials like Ti will require more attention to designing rotors with cooling vents and heat control passages.

Future Plans

Plans to scale up and test thermal spray-coated Ti alloy discs are underway, and the results will be reported during FY 2006.

Table 3. Thermal Conversion Parameter (Q_f) for Various Discs against Jurid 539 (300 N test load).

Disc Material	Q_f (^{o}C/N-m)
Gray Cast Iron	1.18 x 10^{-3}
Ti-6Al-4V* alloy disc	7.30 x 10^{-3}
CermeTi C10*	6.33 x 10^{-3}
Ti-MMC with 5TiB2	3.12 x 10^{-3}
Ti-MMC with (7.5W, 7.5TiC)	3.12 x 10^{-3}
Ti–MMC 10 TiC**	3.75 x 10^{-3}
Red Devil spray-coated Ti*	9 - 10 x 10^{-3}

*Results from FY 2004 studies.
**Similar to C10 but tested with a thinner disc backed by aluminum alloy 3003.

Two new candidate materials, not previously available for friction brake studies, will be evaluated in FY 2006. Both are under development at ORNL. One is an infrared-processed Ti-MMC and the other is a high thermal conductivity, carbon-based composite that is being developed by a novel low-cost processing route.

Publications

P. J. Blau (2000) "Energy Efficiency in Heavy Vehicle Tires, Drivetrains, and Braking Systems – A Multi-year Program Plan," ORNL Technical Report, ORNL/TM-2000/177, 10 pp.

P. J. Blau (2001) "Compositions, Functions, and Testing of Friction Brake Materials and Their Additives," Technical Report, ORNL/TM-2001/64, 29 pp.

P. J. Blau (2003) "Microstructure and Detachment Mechanism of Friction Layers on the Surface of Brake Shoes," *J. of Materials Engr. and Performance*, Vol. 12(1), pp 56-60.

P. J. Blau and J. C. McLaughlin (2003) "Effects of Water Films and Sliding Speed on the Frictional Behavior of Truck Disc Brake Materials," *Tribology International*, Vol. 36 (10), pp. 709-715.

P. J. Blau and H. M. Meyer III (2003) "Characteristics of Wear Particles Produced during Friction Tests of Conventional and Non-Conventional Disc Brake Materials," *Wear*, Vol. 255, 1261-1269.

M. Mosleh, P. J. Blau, and D. Dumitrescu (2004) "Characteristics and morphology of wear particles from laboratory testing of disk brake materials," *Wear*, Vol. 256, pp. 1128-34

J. Qu, P. J. Blau, T. R. Watkins, O. B. Cavin, and N.S. Kulkarni (2004) "Friction and Wear of Titanium Alloys Sliding against Metal, Ceramic, and Polymer Counterfaces," Wear, Vol. 258, pp. 1348-1356.

P. J. Blau and B. C. Jolly (2005) "Wear of truck brake lining materials using three different test methods," Wear, Vol. 259, pp.1022-1030.

P. J. Blau (2005) Research on Non-Traditional Materials for Friction Surfaces in Heavy Vehicle Disc Brakes, ORNL, Tech. Report. ORNL/TM-2004/265, 32 pp.

Conclusions

Studies have been conducted on a wide range of candidate friction brake materials for use in energy-efficient vehicles.

An ORNL technical report has been prepared and distributed to summarize most of the past work on candidate material evaluations.

Research in FY 2005 has revealed the potential of strong, heat-resistant Ti-based metal matrix composites to provide reasonable friction levels. These disc materials tend to run hotter, but the pad material has yet to be optimized to enhance their performance.

Plans are being made to conduct full-scale dynamometer tests on a set of coated Ti-based rotors.

Research in FY 2006 will include two new materials: an IR thermally-processed, in situ formed Ti MMC and a novel carbon composite material, both under development at ORNL.

B. Integrated Approach for Development of Energy-Efficient Steel Components for Heavy Vehicle and Transportation Applications

Co-Principal Investigator: Leo Chuzhoy
Caterpillar, Inc.
P.O. Box 1875, Peoria, IL 61656-1875
(309) 578-6621; fax: (309) 578-2953; email: Chuzhoy_Leo@cat.com

Co-Principal Investigator: Gerard Ludtka
Oak Ridge National Laboratory
P.O. Box 2008, Oak Ridge, TN 37831-6064
(865) 574-5098; fax: (865) 574-3940; email: ludtkagm1@ornl.gov

Co-Principal Investigator: Clyde Briant
Brown University
Box D, Brown University, Providence, RI 02912-D
(401) 863-1422; fax: 401-863-1157; email: Clyde_Briant@Brown.EDU

Chief Scientist: James J. Eberhardt
(202) 586-9837; fax: (202) 587-2476; e-mail: James.Eberhardt@ee.doe.gov
Field Technical Manager: Philip S. Sklad
(865) 574-5069; fax:(865) 576-4963; e-mail:skladps@ornl.gov

Contractor: Caterpillar Corp.
Contract No.: DE-AC05-00OR22726

Objective

This project focuses on development of methods and tools to achieve energy-efficient and environmentally benign steel components. The primary objective of this four-year project is to develop microstructure-level (often called mesoscale) simulation tools (MLS) to capture the formation and influence of nonhomogeneous (real life) microstructures in steel processing. The tools will be used to understand and predict microstructure evolution during processing and ultimately to predict the resultant component performance. This information will then be used to design steel microstructures and develop process roadmaps. The developed techniques will be demonstrated on a pilot project at Caterpillar involving a defined structural component, namely a track roller shaft, which represents a steel component with high production volume that can potentially benefit from microstructure-level improvements. These goals will be achieved through the four tasks described in the technical task section.

Approach

To apply an integrated approach to development of energy-efficient steel components, three major areas of research needs will be pursued:

- Development of microstructure-level models to accurately predict the evolution and behavior of steel microstructures during component processing and performance.
- Characterization of thermo-mechanical properties of microstructural constituents as a function of temperature and composition for exact chemistries.
- Development and integration into the modeling simulation endeavor of the tools to assess required environmental resources.

Accomplishments

Specific MLS modules have been developed and validated for at least one experimental case for the prediction of:

- Solidification microstructures capturing solute segregation;
- Machining damage for each constituent phase as a function of high strain, strain rate, temperature, tool geometry, and loading path;
- The decomposition of austenite during heat treatment for eutectoid and hypoeutectoid steels;
- Accurate stress states and damage in individual phases during heat treatment;
- Microcrack propagation at the fracture initiation stage for the martensite as part of a steel toughness prediction model.

Future Direction

The accomplished MLS machining and casting tasks from the first and second year of this project will be refined during this third year to integrate with the current version of the heat treatment simulation module developed this past year. The phase transformation kinetic model of this heat treatment module developed during year 2 of this project will be also expanded to account for chemical and microstructural inhomogeneities. Likewise, the MLS casting solidification model will be enhanced to predict microporosity along with its current capability to explicitly simulate dendrite growth and alloy segregation. In addition, MLS material strength and fracture resistance models will be developed to explicitly account for inclusions, precipitates, and grain boundaries. Finally, ambient temperature and elevated temperature magnetic processing will be investigated as a material processing approach to tailor microstructures with enhanced performance. Therefore, magneto-thermodynamic processing will be incorporated into the integrated simulation tool as part of the heat treatment considerations for material performance optimization. More specifically, our third year deliverables will be the following:

- A microstructure-level model incorporating phase transformation kinetics that accounts for chemical and microstructural inhomogeneities will be developed and demonstrated for the heat treatment processes used by Caterpillar for the SAE 1045 and SAE 15V45 steel alloys (9/2006).
- Microporosity prediction capability will be incorporated into the casting solidification model (3/2006).
- Experimental failure strain data for individual phases under compressive and tensile loading will be generated for inputs and validation of the damage initiation and failure predictions that will be part of the material strength and fracture resistance model (4/2006).
- The material strength and fracture resistance models will be developed to explicitly account for inclusions, precipitates, and grain boundaries. (8/2006).
- Magnetic processing experiments will be conducted on the ORNL 9-T superconducting magnet to investigate this processing approach for enhancing performance in ferrous alloys of interest to Caterpillar (6/2006).

Introduction

Product cost and performance are two major pressures influencing the acceptance of energy savings technologies by the manufacturers, suppliers, and users in the heavy vehicle and transportation industries. Energy cost has become a significant portion of total product cost for steel applications. Major reductions in energy use are potentially achievable for the transportation and heavy vehicle industries through development and optimization of cost-effective fabrication processes and enhanced product performance.

The key enabling technologies to achieve these benefits are improved materials and realistic, microstructure-level simulations to predict manufacturability and life-cycle performance. Over the past two decades, steel mills and forge shops have successfully implemented numerous energy-efficient processes. The next logical step is to focus

on the development of steel microstructures that are produced in such a way that they are energy efficient and environmentally benign over the entire manufacturing cycle.

Structural materials used in critical steel components of machines have evolved to the point where further improvements in the performance can be achieved only through a fundamental understanding of the mechanisms driving material behavior during processing and service. Microstructural elements such as grain size, inclusion and precipitate distributions, and chemistry control the performance of engineering materials. Variation in these microstructural elements leads to variation in such critical properties as fatigue life, toughness, and wear resistance. Therefore, understanding and developing the capability to control the formation of steel microstructures and predicting the functional and environmental performance is critical to moving the industry closer to its energy-efficiency, resource-efficiency, and pollution-prevention goals. The full realization of these benefits, however, requires a design tool that optimizes the microstructure with respect to the mechanical and environmental performance throughout the life cycle of a particular steel component.

To apply an integrated approach to development of energy-efficient steel components, the development of three major areas of research needs to be completed:

- microstructure-level models to accurately predict evolution and behavior of steel microstructures during component processing and performance,
- thermomechanical properties of microstructural constituents as a function of temperature and composition for exact chemistries, and
- tools to assess required environmental resources.

This project addresses activities required for the first of these three areas. The second and third tasks are either supported by current funding through the National Science Foundation or are expected to be funded through the DOE Initiative for Proliferation Prevention. Through these integrated efforts, a design tool will be developed that optimizes the microstructure, manufacturability, and performance of components with respect to the mechanical and environmental performance required throughout the components' life cycles. The overall benefit of this research will be the development and demonstration of a design methodology that will enable the domestic transportation and heavy vehicle industries to compete effectively in future worldwide markets through improved product performance and energy savings. Furthermore, the proposed design tool can be extended to other materials, i.e., cast iron, aluminum, titanium, magnesium, nickel-based alloys, ceramics, and composites, thus impacting virtually all industries.

In addition to the transportation and steel industries receiving significant energy and cost savings benefit through microstructure-level modeling, virtually all industries will be impacted. Examples of such industries include aerospace (engines, transmissions, structural), marine (engines and drives), agricultural and construction equipment, oil and chemical processing (pumps and gear boxes), military vehicles, mining machinery, appliances (compressors, motors, gear boxes, shafts), power tools, and automotive aftermarket.

Project-end Deliverables

The deliverables for the project will be the following:

- Microstructure-level methods for simulating the manufacturing cycle of steel products coupled with material performance computations (Tasks 1, 2, and 3).
- A specific chemical composition and processing map for a 1500-series steel and a micro-alloyed steel suitable for the application under consideration (Task 4).
- Energy and environmental resources required to produce the selected steel component using at least two steels and processing schemes (Task 4).

The project tasks will focus on three critical areas in the development of these models: heat treatment processing, machining, and materials performance in specific applications. These three processes have been chosen because they are critical steps in reaching the goal of being able to develop a specific steel for a particular application with a heavy

reliance on modeling and with energy requirements optimized as an integral part of the development process. Modeling of casting and forming processing has been performed under other programs, and Caterpillar has shown successful application and commercialization of these models. These existing models will be used along with the heat treatment, machining, and specific applications models described below to complete a suite of models for the manufacture of micro-alloyed steels.

To accomplish the project objectives, a multidisciplinary team consisting of a national laboratory, a university, and a steel end user has been assembled. The team will be supported by an international research institute for material characterization and by experts in environmental impact assessment. The section below describes each of the technical tasks to be performed.

Semi-annual Period Report Topics

Model development and results for the following two topics were reported in detail in the 2005 semiannual report and therefore will not be duplicated in this annual report:

- Solidification microstructures capturing solute segregation
- Machining damage for each constituent phase as a function of high strain, strain rate, temperature, tool geometry, and loading path.

Current Period Progress

Multistage Heat Treat Simulation

Background: Caterpillar started to develop a heat treat simulation package called QSIM in the late 1980s. This predictive tool has gradually become an integral part of heat treat process development, trouble shooting, and material selection in Caterpillar. Recently, an explicit microstructure-based Representative Volume Element (RVE) model was used to capture the mechanical response of steel for different stages of phase transformation. The material response is then used as input for a global model to simulate the quenching process and obtain residual stress during phase transformations. This microstructure level-based simulation approach provided an accurate prediction of material response during heat treat processing. In the current study, the QSIM heat treat simulation is being further integrated into component failure analysis under a multi-scale microstructure based integration model. Microstructure transformations during manufacturing are simulated and are used for material property determination and input to failure analysis. Simulation techniques are being used from initial concept design, through manufacturing process development to failure analysis in a large steel component. The current state of heat treat process simulation and material failure simulation techniques make it possible to accurately predict material behavior and the impact on possible component failure. A combined effect with design, manufacturing simulation and failure simulation will help to address critical issues in the early design stage.

Heat treatment simulation

QSIM contains four modules: (1) a pre-processor for solid model and FEM mesh generation, (2) a quench, carburizing, induction heating, and material database, (3) FEM engines based on ABAQUS, and (4) a post-processor. The database interacts with every major phase of the FEM engines to insure that actual description of the material and quench characteristics are captured. This includes thermodynamics data, transient behavior, phase transformation, related transformation strain and plasticity data, and each individual constituent stress-strain curve under a defined temperature range.

1. Heat transfer model

The temperature field is governed by a standard Laplace equation:

$$\nabla \bullet (k \nabla T) + \dot{q} = \rho c_p \dot{T} \qquad (1)$$

where ρ, c_p, k and $\dot{q}$ are density, heat capacity, heat conductivity and rate of internal heat generation, respectively. The latent heat associated with phase transformations is considered in the model by an enhanced specific heat method. All the material properties are defined as functions of temperature and microstructure.

The most significant factor in transient thermal analysis during steel heat treatment is heat extraction

rate at a part boundary. This heat extraction rate is taken into form as:

$$\left(\frac{dQ}{dt}\right)\Big|_{\Gamma} = h[T(t,x)_s - T_\infty] \quad (2)$$

where Γ is the part boundary, T_∞ is the equivalent ambient temperature, h is the effective heat transfer coefficient, and $T(t,x)_s$ is the time and location dependent surface temperature.

During the quench process, three stages of cooling occur: vapor blanket, boiling, and convection. The three stages of cooling make the heat extraction rate a strong function of part surface temperature, quenchant properties, and the relative velocity of the steel part and the quenchant. Caterpillar has developed a reliable quench characterization method based on measured microstructure and hardness either on a quench characterization bar or on a real quenched component. A genetic algorithm is integrated into the QSIM heat treat simulator to inverse calculate the heat transfer coefficient as illustrated in Figure 1.

The effective heat transfer coefficient is determined by the described quench characterization scheme for the given quenchant and part geometry. It is stored in the quench characterization database and is selected during pre-processing.

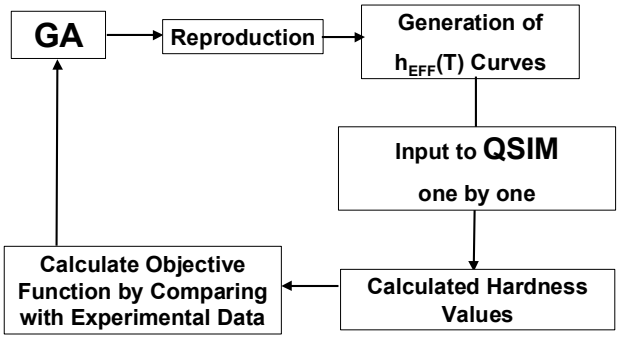

Figure 1. Genetic algorithm (GA) and QSIM inverse heat transfer calculation procedure.

2. Microstructural model

Austenite decomposition is a key element in modeling microstructure formation during the quenching of steel. Many research efforts have been made in describing austenite decomposition kinetics. There are two types of phase transformation involved during heat treatment: diffusion and diffusionless transformations. For diffusion-based transformations, the fraction of the transformed constituent, f_T, is a function of time t, nucleation rate N, and growth rate G. It can be expressed as:

$$f_T(t) = 1 - \exp[-(\pi/3)NG^3t^4] \quad (3)$$

where nucleation rate and growth rate are dependent on temperature, diffusion coefficient of carbon in austenite, free energy barrier and austenite grain size.

For diffusionless transformations, that is when austenite transforms into martensite, martensite-start temperature is first calculated as a function of chemistry. The percentage of martensite is then calculated according to the transformation database deducted from the measured dilatometric curve for each alloy.

3. Stress model

Small deformation theory is applied to heat treat simulation. The total strain in this quasi-static elastic-plastic stress model can generally be expressed as:

$$\dot{\varepsilon}_{ij} = \dot{\varepsilon}^e_{ij} + \dot{\varepsilon}^p_{ij} + \dot{\varepsilon}^{tp}_{ij} + \dot{\varepsilon}^{tr}_{ij} + \dot{\varepsilon}^{th}_{ij} \quad (4)$$

where the superscripts *e, p, tp, tr,* and *th* represent the strain caused by elastic, plastic, transformation plasticity, transformation strain and thermal strain. For multiphase mechanical response, behavior of each individual pure micro-constituent was evaluated from uniaxial tensile tests under various temperatures. An explicit description of microstructure according to volume percentage of each constituent on a normal grain size was used in the micro-scale local model to capture material responses for the global model. Grain boundaries were neglected in this study. For each material within the QSIM database, dilatometric data was also measured for each material to determine transformation strain.

Failure models

1. Material model

The most frequently encoutered mode of failure for heat-treated components is mainly due to void growth and coalescence types of ductile damage processes. Figure 2 shows the ductile dimple type of the fracture surface. This type of fracture normally proceeds in three stages: (1) *void nucleation* by cracking of the particles or decohesion of the inclusions, (2) *void growth* developed by plastic deformation, (3) *void coalescence* by strain localization, void sheet or plastic instability. Different types of models based on micromechanics and damage mechanics have been developed to model these processes. Compared with classical fracture mechanics based approaches, these so-called local approaches do not have geometry dependence and all have certain independency to stress triaxiality. Thus failure parameters can be transferred from lab identification to component level simulation with different geometry and boundary conditions. More important, these models can capture actual mechanisms of failure and supply in-depth understanding of the failure process. Among these void growth models, the Gurson model, which has been modified by Tvergaard and Needleman (GTN), has been proved successful in several studies of lab size failure problems. This modified GTN model can also be combined with other void nucleation and coalescence models.

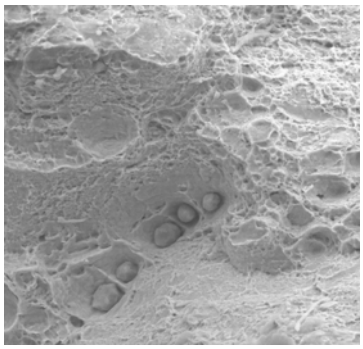

Figure 2. Ductile fracture surface of component. Particles are MnS.

Modifications with considerations like void shape, relative void spacing and strain hardening are also available. Thus, it is chosen for the current study on failure simulation. Due to the element size limitation, the Gurson model has rarely been applied to large component failure simulation. In the current study, the GTN model is used in a submodel manner for failure analysis of a large part.

In the GTN model, flow potential of porous material is given as:

$$\Phi = \left(\frac{\sigma_e}{\sigma_0}\right) + 2f^* q_1 \cosh\left(q_2 \frac{3\sigma_h}{2\sigma_0}\right) - 1 - q_3 f^{*2} \quad (5)$$

Here, σ_0 is the flow stress of non-porous material; σ_e and σ_h are macro-effective stress and hydrostatic stress, respectively; and q_1, q_2, q_3 are parameters to account for void shape and hardening effects. These final three parameters were first introduced by Tvergaard to better fit the curve of a void growth cell model. Interaction of voids near the stage of coalescence can be counted by introducing an effective void volume fraction f^*, which can be expressed as:

$$f^* = \begin{cases} f & f < f_c \\ f_c + \dfrac{f_u - f_c}{f_F - f_c}(f - f_c) & f_F > f > f_c \end{cases} \quad (6)$$

and

$$f_u = \frac{q_1 + \sqrt{q_1^2 - q_3}}{q_3} \quad (7)$$

where, f is void volume fraction, f_c is the critical void volume fraction, and f_F is the void volume fraction at failure. A fixed critical void volume fraction, f_F, at failure is assumed in the model. As the majority of voids formed in the current material are directly from gas porosity, shrinkage porosity and MnS inclusions, voids would form or exist at the beginning of the loading history. Thus, a nucleation stage can be ignored. The increment of f is:

$$\dot{f} = (1 - f)\dot{\varepsilon}_{ii}^p \quad (8)$$

where, $\dot{\varepsilon}_{ii}^p$ is plastic strain increment and follows the summation convention. For Matrix material, an actual hardening curve from mechanical testing has been used.

2. Model parameter calibration

A full Gurson model with consideration of growth and coalescence involves six model parameters. These parameters can be identified with a full curve fit or by combination of micromechanics models and experiment. However, the phenomenological parameters occur in the model regardless of the micromechanics approach. A combined micromechanics and experiment approach was adopted here. q_1, q_2, q_3 are parameters mainly related to void growth, which can be identified by micromechanics study of a cell model by a curve fit manner. Notched bar tests can be used to identify the void coalescence parameters f_c and f_F. Initial porosity volume fraction f_0 is sometimes considered as an adjustable parameter to take the void shape effect into account. In the current study, since most voids and inclusions are spherical, f_0 could be directly identified as the initial porosity volume fraction in the porous material.

Multiscale model integration and failure load identification

To determine the failure load of a component, part assembly structures with applied load need to be analyzed using non-linear contact structure FEM analysis. As discussed in the previous section, part loading capability greatly depends on the residual stress pattern, local material properties, and local material defects. In this study, material properties due to the microstructure difference from heat treatment were mapped into the simulation model. Residual stress was also mapped into the structure assembly. Due to element size restriction, it is difficult and time consuming to directly apply failure models to the global assembly structure.

In the current study, a submodeling technique has been used to identify the global failure load and failure location. First, from global structure simulation, several critical locations were identified as candidates for further submodel micro-scale failure simulation. This can be accomplished by using several criteria based on effective stress, which identifies the plastic deformation, maximum principal stress and a damage stress criterion:

$$\sigma_D = \sigma_e + h\sigma_h \tag{9}$$

where, h is set as 0.4.

Occasionally, large defects might be present in the part due to up-stream manufacturing processes, such as casting. To eliminate those defects can often be very costly and might be unnecessary if not in the critical load carrying locations in the component. It is very crucial to understand how those large defects influence part load carrying capability in order to have confidence in product reliability. These large material defects act like voids normally in the 'mm' size range. Those large material voids could either be predicted using quantitative process simulation tools, or determined by metallurgical investigations. For those locations where large material voids exist in the modeled components, the voids were directly built into the explicitly described micro-scale level local sub-models. Boundary nodes of the sub-model were driven by the global model that carry out the part assembly non-linear calculation. Boundary node reaction force was used to identify global failure load. Small porosity, such as material inclusions, can be treated in the material damage model through initial void volume fraction. Figure 3 illustrated the integration multi-scale modeling scheme used in this study.

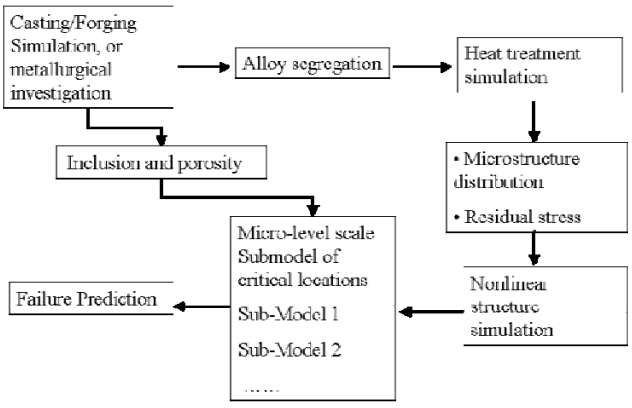

Figure 3. Multi-scale heat-treated component failure analysis scheme.

Application to a Large Steel Casting

A large steel casting weighing 240 pounds and made from low alloy steel was selected to exercise the new model. The part is direct hardened and tempered. Basing cooling rates on previously developed quench characterization techniques, Figure 4 gives the predicted material hardness profile achieved through the direct hardening process. Hardness at surface reached HRC 49 with a fully martensitic structure, while hardness at core only reached HRC 32 with only 30% martensite. The predicted hardness profile was compared with several measured hardness profiles from production parts and is shown in Figure 4. The hardness profile predicted after tempering is also presented in the same plot. The predicted hardness agreed well with the measured curves. As expected, dramatically different material mechanical properties would be formed at those locations due to different microstructure.

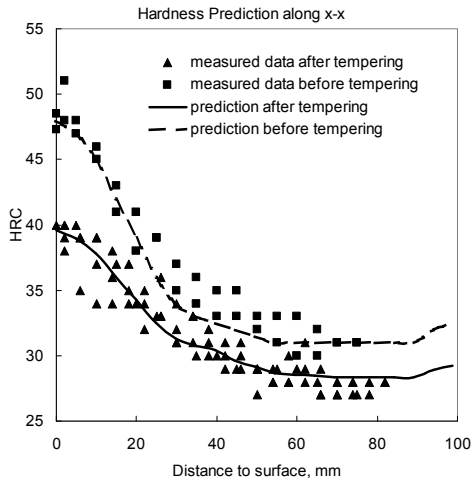

Figure 4. Predicted hardness plot for the large steel casting.

Conclusions

An integrated microstructure level approach has been used for large steel component failure prediction. Simulation started from heat treatment, then results were ported into nonlinear structure simulation and finally to submodeling failure analysis. Final failure load was directly predicted based on heat treat simulation and microstructure porosity inputs. The simulation predictions agreed well with test results. This approach demonstrated that a microstructure-level manufacturing simulation procedure can be used to predict large component loading capacity during the component design validation stage. It can be futher integrated with quantitative material defect prediction models of the various up stream processes to provide a reliable virtual product development and testing platform.

Presentations/Publications/Patents

L. Chuzhoy, C. Briant, A. Needleman, G. Ludtka, "Application of Microstructure-Level Simulation to Life Cycle of Steel Components", presented at MRS Fall 2005 meeting Nov. 28 – Dec. 2, 2005, Boston, MA.

C. Development of Technologies for the Application of Magnesium Metal Matrix Composites for Heavy Vehicles

Principal Investigator: Adam R. Loukus
GS Engineering, Inc.
101 West Lakeshore Drive
(906) 482-1235; fax: 906-482-1236; e-mail: adam.loukus@gsengineering.com

Chief Scientist: James J. Eberhardt
(202) 586-9837; fax: (202) 587-2476; e-mail: James.Eberhardt@ee.doe.gov
Field Technical Manager: Philip S. Sklad
(865) 574-5069; fax: (865) 576-4963; e-mail: skladps@ornl.gov

Participants:
Glen Simula, GS Engineering, Inc.
Andrew Halonen, GS Engineering, Inc.
Josh Loukus, REL Machine, Inc.
Robert Hathaway, Oshkosh Truck Corp.
Chad Johnson, Oshkosh Truck Corp.
Dave Weiss, Eck Industries
Bob Coleman, Engineered Fiber Solutions

Contractor: GS Engineering, Inc.
Contract No.: WR10637

Objective

- Successfully cast magnesium metal matrix composites in an effort to replace low specific strength primary structural components. Implement a selectively reinforced Mg MMC component into a class 8 vehicle.

Approach

- Infiltrate liquid AZ91 magnesium into a variety of readily available ceramic preforms. Evaluate the resulting mechanical and physical characteristics of the samples. The characteristics obtained from an optimum material and process selection shall be used to select and design a primary structural class 8 vehicle component. Once the component is selected, prototypes shall be cast and durability tested. Iterations in design, process, and testing are anticipated prior to successful integration of component on production vehicles. The systematic isolation and control of process parameters is crucial to the success of this project. The team has worked with production squeeze casting and pressureless infiltration processes and found them inadequate from a process control standpoint. This has resulted in an effort to design a state of the art process-controlled squeeze casting press.

Accomplishments

- Accomplishment 1 – Cast samples exhibiting elastic moduli three times that of as-cast AZ91D (from 6.5 to ~20 Mpsi).

- Accomplishment 2 – Acquired extensive knowledge in casting magnesium composites through hands on trials and literature search.
- Accomplishment 3 - Developed in-house casting capability with the focus of extensive process control.

Future Direction

- Milestone 1 – Refine material, i.e. matrix/reinforcement, and process parameters for production capable system.
- Milestone 2 – Select, design, cast, test, implement component(s) for heavy duty specialty trucks.

Introduction

Metal matrix composites (MMCs) have been the focus of numerous studies based on the promise of high specific strength and modulus. Weight savings, without loss in performance, has provided a driving force to develop MMCs using various reinforcements. Preforms of silicon carbide particles and/or whiskers, (SiCp and SiCw), Al_2O_3 particles and/or fibers, carbon fibers, and hybrid combinations of these when used in conjunction with high pressure casting processes that infiltrate the perform with molten metal have specific component design and production advantages. The incorporation of a hard, high modulus reinforcement into a malleable metal matrix provides an end product with properties predictable through the rule of mixtures. Preforms in conjunction with squeeze casting offer selective reinforcement versus a random distribution common in stir casting. Squeeze casting densifies the casting to reduce porosity and grain size thereby maximizing ductility and toughness for a given strength and stiffness. Squeeze casting, powder metallurgy, spray deposition and stir casting methods are commonly used in industry to produce MMC materials. (Gui et al 2004,Kaneko et al 2000, Chmelik et al 2000)

The use of magnesium alloys in the production of MMCs is of interest for researchers and industrial professionals due to the low density of the material and a relatively high stiffness to weight ratio. For example, a common magnesium alloy, AZ91 has a density of 1.81g/cc, whereas aluminum alloys and steel densities are 2.7 and 7.8g/cc respectively.

The focus of this work investigates the potential of using magnesium MMCs in stiffness, strength, and wear driven applications. There have been numerous investigations into this area especially with aluminum alloys. Magnesium composite studies, while not so thoroughly researched as aluminum, have been performed and have provided the impetus and direction to the current investigation. The goal of the first portion of the work is to quantify and reproduce material properties to understand strength mechanisms and matrix/reinforcement interactions in magnesium composites. In the larger scope of the work, components of Mg MMCs could be implemented into Class 8 vehicle components.

Figure 1 illustrates the constraints, variables and goals of the projects. The funding, time and resources are fixed to reach the high strength, weight reduction (HSWR) goals. The design, mechanical properties, quality, cycle time and cost of the resulting component are affected by the process. The selection of an optimized process with control of as many process parameters as possible will result in consistent high quality components. As consistency increases, the overall yield of a given melt will increase resulting in lower overall product cost. In the final analysis cost is the driver in whether a material/technology is introduced on a vehicle platform.

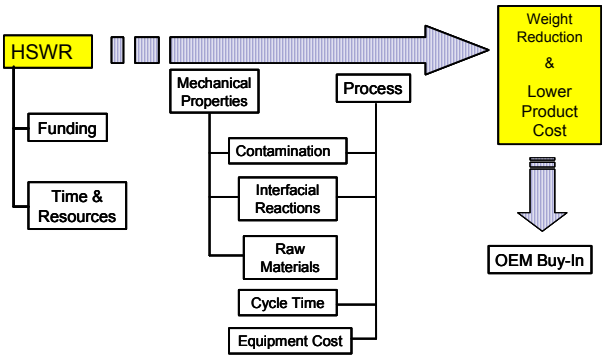

Figure 1. Flow chart of objectives and variables affecting mechanical properties and outcomes.

Carbon fiber work, performed by Schultz et al 1999, demonstrates the effect of pressure during the infiltration of a preform. A pressure-tight inert autoclave is used in the experiment as the casting press. The pure magnesium (99.95%) matrix material and the preform are heated in a vacuum until the melting point of the matrix is achieved. The vacuum is then broken and Argon (Ar) gas is allowed to flow into the chamber to prevent oxidation. The autoclave produces the pressure needed for the molten metal to infiltrate the space within the permeable carbon fiber preform and the densifying force needed to minimize shrinkage porosity. For a given carbon fiber perform, both aluminum and magnesium trials showed the resulting flexural strength and flexural modulus of the MMC were directly related to applied pressure (up to 40 MPa) during infiltration.

Alumina, Al_2O_3, is a widely used preform material and has been utilized extensively in aluminum and magnesium work. Creep tests performed on magnesium reinforced with Saffil fiber at a 20% volume fraction (vf) showed increases in creep resistance, strength and stiffness over the monolithic alloys in the study. (Sklenicka et al 2000).

Perhaps the most prevalent preform material in the literature is silicon carbide. Silicon carbide particles promote higher modulus and wear resistance with moderate increases in strength (Zheng et al 2000, Svoboda et al 2000, Gui et al 2004). Silicon Carbide whiskers have also been used for similar mechanical property enhancements (Kaneko et al 2000, Zheng et al 2004). Typical whisker aspect ratios are from 10 to 100. The prior art shows that the volume fraction of reinforcement is directly related to elastic modulus, wear resistance and ultimate tensile strength. This is true for both the particulate and whisker reinforcement morphologies.

As in the case of common engineering materials, increases in strength and stiffness come at a cost to the ductility and toughness of the material. The higher the strength and the stiffness, the lower the failure strain for a given composite. The successful integration of MMCs in vehicle component design requires a thorough understanding of this mechanical property tradeoff. On the other hand this tradeoff can be tailored through modifications in the interfacial reactions that take place between the fiber and matrix materials. (Kaneko et al 2000, Zheng et al 2004). The preform binders that coat the material react to produce by-products that can be favorable or unfavorable for load transfer between the matrix and the reinforcing material. Kaneko performed tests with whiskers that were uncoated and observed fracture along the whisker matrix interface due to the lack of interfacial reactions. When a silica binder was used to coat the whiskers the magnesium wetted the reinforcement enabling the formation of interfacial MgO which bonded the matrix to the whisker. Different types of binders such as $Al(PO_3)_3$ are available and offer different reactions for binding the composite constituents (Zheng et al 2001, Zheng et al 2003).

Background

AZ91D Precipitation Behavior:

Theory states that AZ91D contains a nominal 9% Al and 1% Zn and a small amount of Mn (0.15%). Based on the binary Mg-Al phase diagram, under equilibrium conditions, this alloy will solidify as a single phase α-Mg solid solution and subsequent cooling will lead to the precipitation of an inter-metallic $Mg_{17}Al_{12}$ (β-phase) within the α-Mg grains.

In reality, in commercial casting operations, faster cooling rates will cause non-equilibrium cooling conditions which will lead to the formation of eutectic consisting of α-Mg solid solution and $Mg_{17}Al_{12}$ (β-phase). As the temperature cools below the liquidus, the α-Mg (primary) will begin to solidify and grow. As the temperature decreases toward the eutectic temperature, the liquid becomes enriched in aluminum because the solid that forms will contain a lower amount of Al than the nominal composition since there is not enough time for diffusion to take place in the solid. As the remaining liquid reaches the eutectic temperature, it solidifies as two phases: supersaturated α-Mg and $Mg_{17}Al_{12}$. Therefore, at room temperature, the alloy will contain three phases: Primary α-Mg, eutectic α-Mg and $Mg_{17}Al_{12}$.

Solution heat treated (T4)

Solutionizing requires bringing the solidified alloy to a temperature above the solvus line and holding there until the $Mg_{17}Al_{12}$ phase is dissolved and a

homogeneous α-Mg solid solution is formed. Subsequent quenching retains the single α-Mg phase, but now the phase is super-saturated i.e., there is excess aluminum in a non-equilibrium state.

The ASTM (ASTM B 661) recommended heat treatment for AZ91 casting alloy is 775°F for 16 to 24 hours. ASTM also suggests an alternate treatment to minimize grain growth; a) 775°F for 6 hrs.; b) 665°F for 2 hrs.; or c) 775°F for 10 hrs. It is possible that the optimum solution treatment for squeeze cast composites will have a shorter time because the $Mg_{17}Al_{12}$ will be more broken up and therefore require less time to dissolve into the matrix.

Aging treatment (T6)

Aging the T4 structure at a temperature below the solvus will allow the excess aluminum to diffuse to nucleation sites and form $Mg_{17}Al_{12}$ precipitates. Since these precipitates are formed at a lower temperature compared to the eutectic $Mg_{17}Al_{12}$ formed during solidification, they will be finer and more evenly dispersed and therefore more effective at strengthening the alloy.

The ASTM recommended aging treatment for an AZ91 casting is a) 335°F for 16 hrs. or b) 420°F for 5-6 hrs. It is likely that the optimum aging treatment will be different for a composite. Jayalakshmi et al., found that the presence of ceramic reinforcements significantly decreases the peak aging time for an AM100/Saffil short fiber composite. It is suggested that the presence of the fiber-metal interface provides nucleation sites and enhances the precipitation.

Effect of the preform

Table 1 summarizes the reactions that can take place between the matrix and the ceramic/preform binder. The interfacial reactions that take place can enhance or degrade the desired mechanical and physical characteristics of the composite. The goal is to form a strong bond between the ceramic and matrix without forming detrimental reaction products at the interface. Although the interface reactions can increase the ability of the matrix to wet the ceramic, the reaction products or a chemical degradation of the ceramic can adversely affect the mechanical properties of the composite. A method that minimizes reaction product but achieves matrix to fiber load transfer under stress is the balance that must be achieved in the production of a quality engineering material. This is the approach taken by the Lo et al patent. By forming a coating of magnesium fluoride on the surface of the ceramic, the interfacial reactions are avoided.

Table 1. Possible interfacial reactions that can form with an Mg + Al alloy:

Ceramic or binder	Possible Interfacial Reactions:
C	$4Al + 3C \rightarrow Al_4C_3$
Si	$Si + 2Mg \rightarrow Mg_2Si$
SiC	$4Al + 3SiC \rightarrow Al_4C_3 + 3Si$
Al_2O_3	$3Mg + 4\ Al_2O_3 \rightarrow 3Mg\ Al_2O_4 + 2Al$ $3Mg + Al_2O_3 \rightarrow 3MgO + 2Al$
SiO_2	$Mg + 2SiO2 + 2Al \rightarrow MgAl_2O_4 + 2Si$ $2MgAl_2O_4 + 3Si \rightarrow 2MgO + 3SiO_2 + 4Al$ $2Mg + SiO_2 \rightarrow 2MgO + Si$

Procedure

Squeeze Casting

A vertical squeeze cast press was utilized in this work. The machine specifically was a 400 ton model with an H-bar die. Figure 2 shows pictures of this equipment. In this method the material can be injected and held at 100 MPa in order to reduce both the infiltration porosity and the shrinkage porosity. This is a commercially viable process with potential for high volume production quantities. The following is the procedure for infiltration and Table 2 shows the process parameters.

1. Shot Sleeve Charged with Liquid Magnesium.
2. Preforms were preheated to 1292°F and placed into the die cavity.
3. Die is slid into position.
4. The die is closed and clamped together with 400 tons of closing force.
5. Shot piston moves up, forcing material into the die and preforms at a predetermined speed.
6. Pressure is held until solidification of the casting.
7. Die opens and the part is taken out.

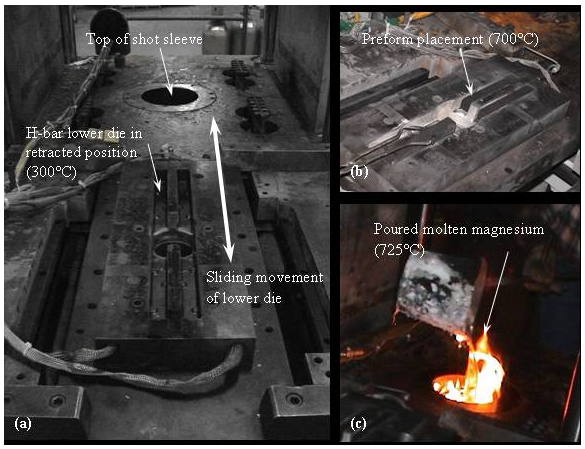

Figure 2. (a) Squeeze casting equipment with an H-bar die with (b) preforms inserted. (c) molten magnesium poured into shot sleeve.

Table 2. The process parameters set for these tests.

Process parameters	Value
Molten Magnesium Temperature (°C)	725
Die Temperature (°C)	300
Shot Speed (in/sec)	1
Shot Time (sec)	4.5
Pressure (psi)	3000
Dwell (hold) Time (sec)	100
Reload Time (sec) (approx.)	150
Total Cycle Time (sec)(approx.)	255

The squeeze casting trials with the H-Bar die resulted in samples contaminated with MgO inclusions. As a result, it was imperative to eliminate the opportunity for MgO inclusion formation. It was felt the majority of the oxidation took place during transfer of the liquid magnesium to the shot sleeve. The liquid must be protected during this step to provide consistent properties within a given Mg MMC system.

Pressureless Infiltration

A comparative study was performed on similar materials using a pressureless infiltration method. The pressureless infiltration furnace enables the process to take place within a specialized casting atmospheres. The inert cover gas allows the liquid to infiltrate the preform without competing with oxidation reactions. This process eliminates the need for an expensive die because the preform is infiltrated largely by capillary action. The preform is placed on top of the magnesium in the furnace as it melts. Figure 3 illustrates this pressureless infiltration process.

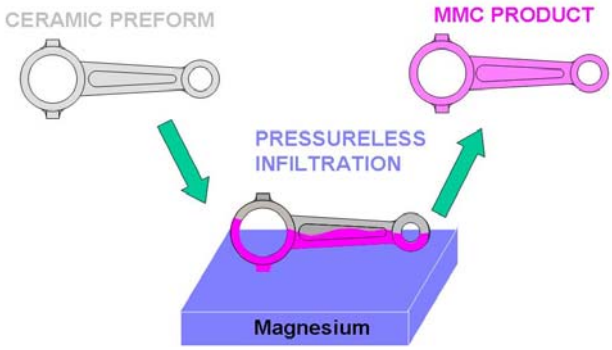

Figure 3. Schematic of the pressureless infiltration process.

This process is effective for near net shaped reinforcements involving complicated geometry and better melt flow. The disadvantage of this casting method is that it is slow and difficult to achieve high cooling rates needed for solid solution strengthening (Polmear, 1995).

A simplified procedure follows:

1. Set preform down in graphite bedding material
2. Magnesium billet placed on top
3. Argon purges chamber
4. Ramp furnace to desired temperature with argon flow through furnace
5. Alloy melts and completely infiltrates preform
6. Furnace cooled to 400ºC ***(Units)*** with argon flow
7. Break away bedding material and extract finished part.

Preforms of various types were cast using this method. AZ91D and AZ91E alloys were used for these trials. The resulting mechanical properties are discussed in the following results section.

PIVAC Method

The PIVAC (Pressure Infiltrated, Vacuum Assisted Casting) method was specifically designed for infiltrating preforms with liquids. Experiments conducted were well instrumented to monitor the temperature and pressure inside the die. Two thermocouples were placed in the region where the magnesium billet sits and three thermocouples were placed along the length in the preform region shown in Figure 4.

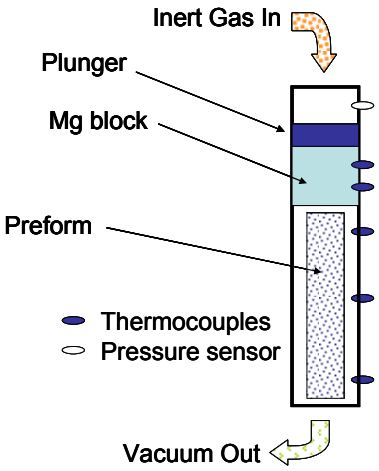

Figure 4. PIVAC method schematic.

The temperature is monitored during the critical stages of the process. The method is similar to the carbon fiber work performed by Schultz et al 1999, which demonstrated the affect of pressure during the infiltration of a preform. A pressure-tight inert autoclave is used in the experiment as the casting press. The pure magnesium (99.95%) matrix material and the preform are heated in a vacuum until the melting point of the matrix is achieved. The vacuum is then broken and Argon (Ar) gas is allowed to flow into the chamber to apply pressure to the matrix material. This pressure, combined with the vacuum forces the molten metal to infiltrate the carbon fiber preform and minimize shrinkage porosity. The flexural strength and the modulus both increased as a function of pressure (up to 40 MPa) during the casting trial for both magnesium and aluminum for a given carbon fiber preform material (Shultz, et al. 1999). The experimental lab setup used for this work is shown in Figure 5.

The experimental procedure is as follows:

1. Place preform and 2” diameter magnesium billets in die cavity with plunger. Close die.
2. Bolt together top and bottom die.
3. Attach thermocouples, vacuum and argon pressure lines to die.
4. Place die in furnace and bring temperature up to 1200°F (monitor thermocouples with data acquisition system. Vacuum die chamber simultaneously.

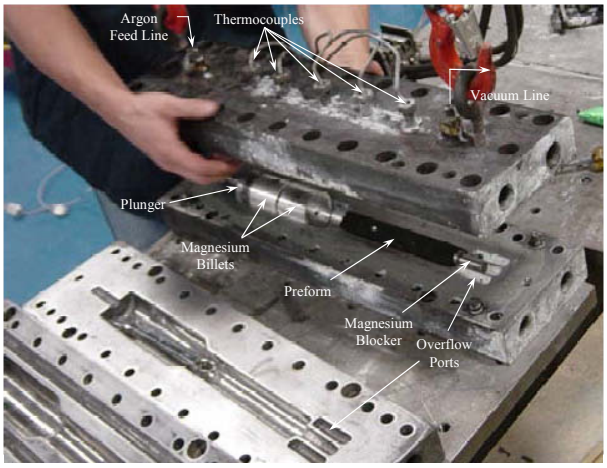

Figure 5. Experimental setup of the PIVAC method.

5. Once temperature is reached in the die. Apply argon pressure to specified value.
6. Open furnace, force air cool to 900°F, quench in water to room temperature.
7. Unbolt dies and remove infiltrated preform.

Results and Discussion

There are several data sets that could be compared from the three different processes, Squeeze Casting, Pressureless and PIVAC. In the current study, the tensile strength, elastic modulus and strain to failure were measured. The data from the different processes is tabulated below.

Squeeze casting gave good results when filters were incorporated to limit MgO inclusion contamination. Results from the trial are tabulated below.

The non reinforced AZ91D squeeze cast control run results provided properties consistent with published data. Squeeze casting with single constituent preforms and hybrids of mixed fibers and particulate placed in the H-Die prior to infiltration was performed. The results from these tests showed various degrees of success. With the exception of O influence affecting repeatability, the data below indicates the promise of using a squeeze cast machine in producing composite components, specifically those with hybrid preforms.

Table 3. AZ91D Squeeze Cast Material Properties

Condition	Ultimate Tensile Strength (UTS)	Strain at UTS (%)
As Cast	21100 psi (145 MPa)*	1.2*
T6	29850 psi (206 MPa)*	2.7*
	*average of 5 tests	

The hybrid preforms were the most successful under the process conditions chosen for these studies. These showed great gains in elastic modulus when compared to the non reinforced control. Figure 6 demonstrates the production potential of this process for composite material manufacturing. However, there are negative attributes in the composite material properties due to lack of complete infiltration, compaction and fracture of preforms and the deleterious effects of MgO formation.

The squeeze cast trials were run on a production caster which did not have access to monitor and control the parameters that were felt necessary for the production of a consistent quality composite material. A more in depth understanding of the fluid dynamics and chemical reactions is essential. More controlled infiltration studies to understand the reactionary chemistry of the process was undertaken.

Pressureless infiltration studies were performed at GOM Technologies in order to understand the infiltration potential of various preform materials. Using the pressureless process would also provide evidence on the effects of infiltration velocity and cooling rate on material properties. The controllable casting atmosphere in the process eliminates rapid oxide formation prevalent with the squeeze casting process. The matrix material in the pressureless infiltration studies and the PIVAC process showed much lower matrix strengths as shown in Table 4 below. It is felt that the lower cooling rates contributed to large grain size (Figure 7).

Although the grain size has an adverse affect on the mechanical properties of the castings, the strength of carbon fiber Mg MMC more than doubled the matrix material strength. The strain to failure increased as well. This indicates that there is good

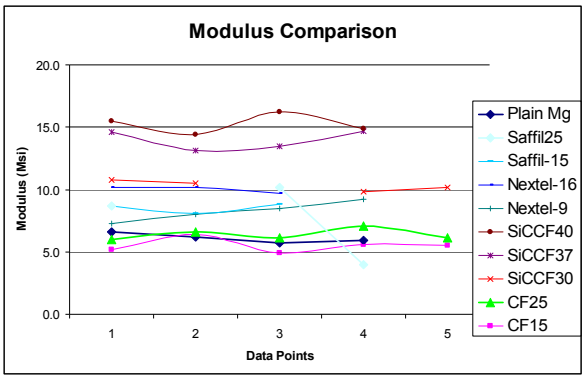

Figure 6. Squeeze Cast composite modulus data

Table 4. Pressureless Infiltration Data

Material	Elastic Modulus (Mpsi)	Elastic Modulus (GPa)	UTS (psi)	UTS (MPa)	Strain at Failure
33% SiC - 4% Carbon Fiber	19.5	134.4	29000	199.9	0.0021
33% SiC - 4% Carbon Fiber	17.9	123.4	24900	171.7	0.0019
33% SiC - 4% Carbon Fiber	14.2	97.9	27400	188.9	0.003
33% SiC - 4% Carbon Fiber	22.3	153.8	34900	240.6	0.003
Saffil - 15	15.7	108.2	11500	79.3	0.007
Saffil - 15	12.9	88.9	13300	91.7	0.0015
Saffil - 15	10.5	72.4	15200	104.8	0.0019
Nextel - 9	7.95	54.8	14200	97.9	0.0028
Saffil - 15	8.75	60.3	14900	102.7	0.0034
Nextel - 9	8.25	56.9	10500	72.4	0.0017
54% alumina	15.31	105.6	10450	72.1	0.00213
54% alumina	N/A	N/A	10550	72.7	N/A
54% alumina	16.3	112.4	14950	103.1	0.00092
CF - 25 AZ91E	N/A	N/A	19050	131.3	0.00415
CF - 25 AZ91D	N/A	N/A	21700	149.6	0.00361
CF - 25 AZ91D-1	N/A	N/A	25885	178.5	0.0086
CF - 25 AZ91D-2b	9.8	67.6	31107	214.5	0.0089
CF - 25 AZ91D-3	N/A	N/A	32189	221.9	0.0049
CF - 25 AZ91E-4b	N/A	N/A	27708	191.0	0.0063
CF - 25 AZ91D-5b	11.2	77.2	34353	236.9	0.009
CF - 25 AZ91E-6	3.86	26.6	11812	81.4	0.0048

Figure 7. AZ91D fracture surface - PIVAC method.

Table 5. PIVAC experimental data

Material	Elastic Modulus (Mpsi)	Elastic Modulus (GPa)	UTS (ksi)	UTS (MPa)	Strain at Failure
CF 15 - 1	5.67	39.1	31.6	217.9	0.0110
CF 15 - 2a	6.96	48.0	35.2	242.7	0.0084
CF 15 - 2b	5.16	35.6	16.7	115.1	0.0045
CF 15 - 3a	7.51	51.8	27.4	188.9	0.0096
CF 15 - 3b	6.01	41.4	27	186.2	0.0071
CF 15 - 4a	6.31	43.5	25.9	178.6	0.0086
CF 15 - 4b	6.17	42.5	23.5	162.0	0.0068
CF 15 - 5	5.51	38.0	25.6	176.5	0.0093
CF 15 - 6	5.05	34.8	22.3	153.8	0.0085
Pure AZ91E - 7	N/A	N/A	12.7	87.6	N/A
CF 15 - 8a	N/A	N/A	26.03	179.5	N/A
CF 15 - 8b	N/A	N/A	25.96	179.0	N/A
CF 15 - 9_1	6.8	46.9	24.54	169.2	0.0088
CF 15 - 9_2	6.11	42.1	14.48	99.8	0.0031
CF 15 -10	9.29	64.1	24.4	168.2	0.0073
CF 25_1	7.65	52.7	11.79	81.3	0.0022
CF25_1b	12.1	83.4	20.1	138.6	0.0038
CF25_2	7.96	54.9	17.32	119.4	0.0031
CF25_3	13	89.6	23.07	159.1	0.0045
CF25_4	7.55	52.1	20.98	144.7	0.0049
CF25_4b	5.31	36.6	20.24	139.6	0.0031
AZ91E_1	5.82	40.1	12.06	83.2	0.0035
AZ91E_2	3.03	20.9	6.4	44.1	0.004
CF25_1	5.19	35.8	27.05	186.5	0.0061
CF25_3	9.28	64.0	26.99	186.1	0.0056
CF25_4	6.57	45.3	26.13	180.2	0.0054

CF 15 - Averages	6.41	44.17	23.97	165.28	0.0074
CF 25 - Averages	8.29	57.16	21.52	148.37	0.0043
AZ91E - Averages	4.43	30.51	10.39	71.61	0.0038

adhesion and load transfer between the matrix and the carbon fiber reinforcement

The PIVAC elastic modulus for the Mg MMC with the SiC_p-C_f hybrid preform is similar to that observed with the squeeze cast trial. This suggests that casting in an inert environment can bolster the mechanical properties without the implementation of high pressures (in a dense preform).

The effects of pressure on the results from the PIVAC method were not able to be delineated in the study due to leakage problems in the die. The pressure was then reduced in order to keep the molten magnesium contained to minimize collateral damage. However, calculations of material infiltration based on weight show that the preform was fully infiltrated. This pressure affect and effects of heat treatment will be further pursued in future work to set process parameters in future squeeze cast trails. Also, metallographic, SEM-EDS, and TEM characterization of matrix-reinforcement interfacial reactions are ongoing.

Microstructural Analysis

Due to the reactive behavior of the magnesium melt, the reactions between the molten metal and the reinforcement need to be analyzed. Extensive work was done analyzing the preform-metal interface. The microstructural features affect the macroscopic response (yield strength and UTS) and therefore it is important to control the reactions at this interface. The following SEM micrograph (Figure 8) of a fracture surface from a squeeze casting sample shows the fiber-matrix interface. It can be observed that the bond strength in this sample is poor as there are areas of fiber pullout. This is reflected in the poor mechanical properties of the material as the fibers are pulling out of the matrix and the load transfer is poor due to this adhesive failure.

SEM observations from the samples cast in an inert environment during pressureless infiltration show a different behavior. It is shown in Figure 9 that the fibers are cracking and the fracture of the material is shearing through the fibers rather than pulling them out. This is an example of cohesive failure. This is the mode in which increases in strength and moduli are seen.

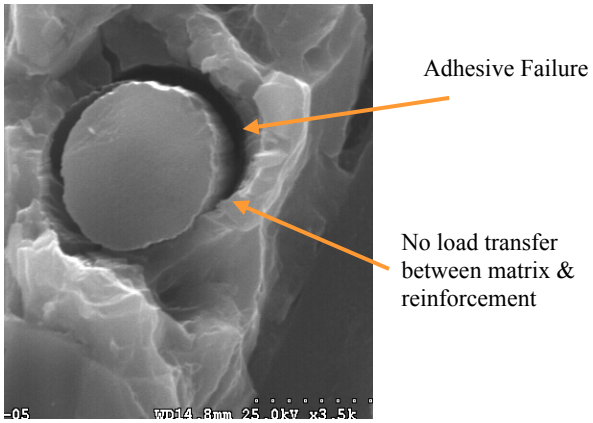

Figure 8. Adhesive failure between the fiber and the surrounding magnesium matrix.

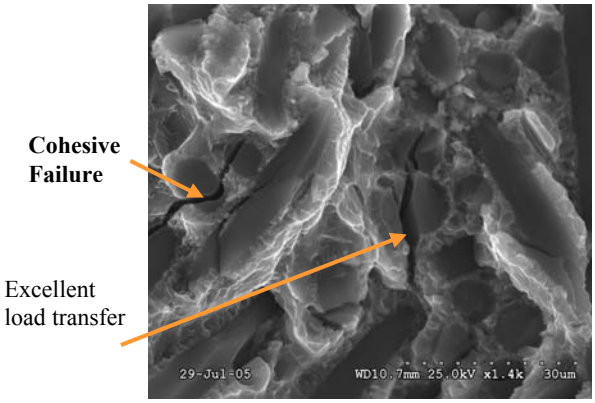

Figure 9. Cohesive failure of the material showing an excellent bond between the fibers and matrix.

Squeeze Casting Press Development

From the above casting iterations, it is clear that there is a distinct need for process control and the correct process selection. Each process brings its own set of variables, advantages and disadvantages. Figure 10 shows how each affects the end goal of achieving excellent metallurgical and mechanical properties.

It is well known that a fine grain structure leads to improved mechanical properties. Therefore, the squeeze casting process looks favorable due to the inherent fast solidification rates leading to fine grains. Squeeze casting also reduces the casting cycle times, and therefore, reduces part cost. The inert environment seen by the pressureless infiltration process shows that casting without MgO

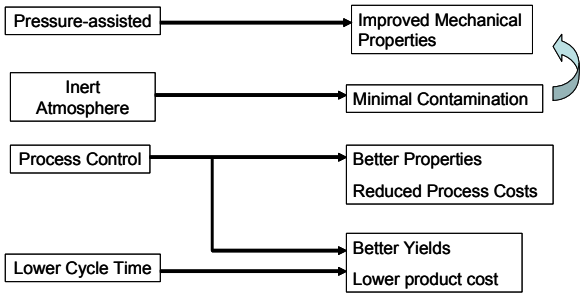

Figure 10. Positive attributes of each process.

contamination can dramatically improve the mechanical properties of the Mg MMC. If the process parameters are carefully controlled, the mechanical properties are favorable. The detrimental affects of pressureless infiltration are seen when the fibers degrade due to long reaction times between the magnesium alloy and the reinforcing fibers.

It is of great scientific and commercial interest to combine the positive attributes of each of these processes to cast components. Therefore, the intent of the PIVAC method was to prove this concept. The results have shown that there is promise in this ideology, and therefore a squeeze casting press is being built specifically with these factors considered.

Most commercial squeeze casting presses available today have some exposure of the melt to the air. The intent of this press is to control the environment completely throughout the casting process. Other improvements are extensive process control. Careful monitoring and control of melt temperature, preform temperature and shot sleeve temperature; shot velocity, profiles and pressure are very important to control to avoid damage to the preforms, yet obtain complete infiltration.

The press (Figure 11) has a 400 ton capacity with the potential of providing ~15000 psi (~100MPa) of pressure to the molten metal. Process control and melt protection are crucial design criteria.

Preliminary casting trials will commence in early December 2005.

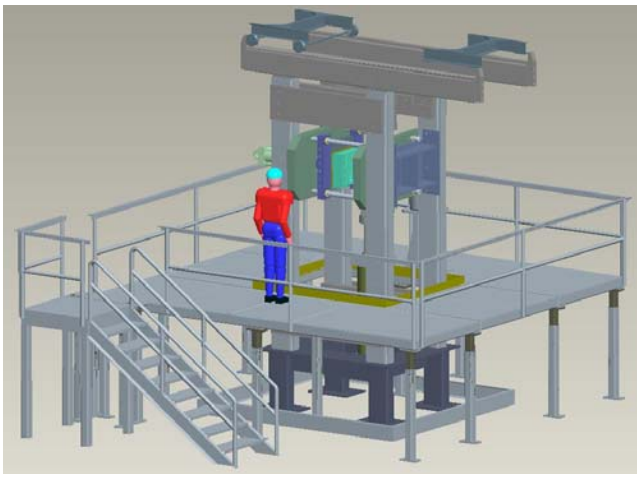

Figure 11. 400 ton squeeze casting press.

Conclusions

Process control in magnesium metal matrix composites is complicated by the reactive nature of the molten metal. Interactions between the metal and the preforms can be positive for good fiber-matrix bonding, but too much of these reaction products can produce intermetallics and oxides that are unwanted in the matrix.

New process development is underway to cast selectively reinforced magnesium composites. Component casting and testing will occur in the early part of 2006.

Presentations/Publications/Patents

1. ORNL – Heavy Truck Peer Review. Status of "Development of Technologies for the Application of Magnesium Metal Matrix Composites for Heavy Vehicles" Sept. 13, 2005.
2. AFS International Conference on High Integrity Light Metal Castings. "The Effects of Processing Methods on the Mechanical Properties of Cast Magnesium Metal Matrix Composites." Oct. 31 – Nov. 1, 2005. Indianapolis, IN.
3. TMS – Rohatgi Honorary Solidification Symposium of Metal Matrix Composites; "Solidification Rate Effects on Microstructural and Mechanical Properties in Pressure Cast Magnesium Metal Matrix Composites." March 12-16, 2006 in San Antonio, TX.
4. NADCA, 110th Metal Casting Congress, April 18-21, 2006. Mg MMC topic. Columbus, OH.

D. Lightweight Functional Composite Materials

Principal Investigator: Nidia C. Gallego
Oak Ridge National Laboratory
P.O. Box 2008, Oak Ridge, TN 37831-6087
(865) 241-9459; fax: (865) 576-8424; e-mail:gallegonc@ornl.gov

Chief Scientist: James J. Eberhardt
(202) 586-9837; fax: (202) 587-2476; e-mail: James.Eberhardt@ee.doe.gov
Field Technical Manager: Philip S. Sklad
(865) 574-5069; fax:(865) 576-4963; e-mail: skladps@ornl.gov

Participants:
Dan D. Edie, Clemson University
Edwin H. Kraft, EHK Technologies

Contractor: Oak Ridge National Laboratory
Contract No.: DE-AC05-00OR22725

Objectives

- To develop an economic evaluation of the cost of providing fuel to internal combustion engines using ORNL's carbon fiber monoliths as a medium for storing adsorbed natural gas for use in vehicular applications.
- To investigate and develop methodologies to disperse metal nanoparticles in a carbon fiber substrate and, to determine the appropriate heat treating (stabilization and carbonization) and activation conditions for metal-containing fibers.

Approach

- Prepare process flow diagrams for monolith and storage system manufacture.
- Create an economic model for the methane storage and delivery (tank to engine, including injection) system.
- Determine cost of vehicular methane pressure storage and gasoline storage and delivery systems.
- Determine operating fuel cost of gasoline and methane systems in comparable vehicles.
- Mix metal salts with isotropic pitch, the precursor for carbon fibers; initial run will evaluate palladium additions.
- Melt-spin metal-containing pitch into fiber form. Stabilize, carbonize, and activate metal-containing fibers.
- Characterize surface area and pore size distribution of metal-containing carbon fibers.

Accomplishments

- Economical model showing that high cost of precursor carbon fiber, makes ORNL's monolith an extremely expensive material for storing adsorbed natural gas.
- Successfully melt-spun carbon fibers containing approximately 1 wt % of the following metals: silver, palladium, and silver/palladium mixtures. These samples were heat-treated (stabilized and carbonized) and activated to developed porosity.

Future Direction

- The development of low cost carbon fiber is a critical step towards reducing the cost of carbon fiber monoliths. The low cost carbon fibers could increase the potential of carbon fiber monolith as a medium for storing adsorbed natural gas at low pressure.
- Metal-containing carbon fibers have potential application for enhanced gas storage and catalysis applications, however, the evaluation of these applications are not part of the scope of this program and will not be pursued further here.

Introduction

During this fiscal year, we undertook two main tasks in this project: The first one was to conduct an economic analysis of the cost of using ORNL's carbon fiber monoliths for storing adsorbed natural gas for vehicular applications; this task was carried out by EHK Technologies under contract with ORNL. A summary of the findings is presented below. A more detailed report of this economic evaluation is available upon request.

The second task was to investigate methodologies for the production and processing of metal-containing activated carbon fibers. This task was conducted in collaboration with Clemson University.

Cost Model - Introduction

Natural gas is currently used as an alternative fuel in vehicles such as taxicabs, buses and some medium duty trucks. The method of fuel storage in each of these cases is as a compressed gas in what is essentially a pressure vessel. This gas is stored in most cases at 250 bar (3,600psi). An alternative storage concept consists of using ORNL's carbon fiber monolith, capable of adsorbing natural gas in large volumes at considerably lower pressure. In concept, this new method would have the advantages of lower cost and lighter weight for the storage equipment.

The present study was conducted to assess the cost and weight of this Adsorbed Natural Gas (ANG) system compared to the conventional Compressed Natural Gas (CNG) system. The intended application for this ANG system is medium duty trucks at a rate of 50,000 units per year.

Approach and Results

The cost of manufacture of an ANG storage system was estimated by creation of a mass production concept and economic model of that production. The concept was based on the limited data available from laboratory material, process and application experiments conducted at ORNL. Laboratory data on material composition, processing and methane storage capacity was necessary to calculate material volume requirements and process parameters. Early in this study, it became apparent that the method of producing ANG storage material used in the lab efforts would not be suitable for production of the large quantities required by the intended application. A high volume production methodology was therefore conceived based on discussion with both ORNL personnel and manufacturers of process equipment applicable to several potential methodologies.

The essential difference in use of ANG vs. CNG as a fuel system for vehicles is only in the storage tank and media. Vehicles would use natural gas at the same pressure, and with the same delivery and carburetion system regardless of how the gas was stored, and would require pressure and flow regulators of approximately the same cost regardless of the storage pressure. The essential difference in cost is therefore the cost of tank and storage media. The amount (mass and volume) of ANG storage media therefore became a critical study parameter. A key issue in determining this requirement is the storage capacity of the media at a reasonable pressure.

Previous work at ORNL showed that the "deliverable capacity" of the media with an average density of 0.65 g/cc, was 120 (V/V). V/V is the volume of gas at 500 psi per unit volume of media. This means that for this study, we assume that at 500 psi, the media will store 120 times its gross volume of methane.
Using the data collected and reasonable assumptions, the cost of an ANG storage device would be approximately $10,000, and the device would weigh approximately 1,100 lbs. The breakdown of cost and sale price is shown in Figure 1. Obviously, the car-

bon and resin raw materials at 60%, and the steel shell of the container at 20%, constitute the majority of expected price of this device.

Conclusions

The results of the technical and economic analysis provided an estimate of the production cost of an ANG storage system and comparison to a CNG system. A CNG storage tank for a 20 gallon gasoline equivalent is about 60 gallons in volume, and would cost from ~$250 for Type 1 all steel weighing ~200lbs, to over $2,000 for a Type 4 all composite tank weighing only about 100lbs. Thus, saving around 100lbs of weight costs close to $2,000. The penalty in space of using CNG vs. gasoline is a factor of 3X. An ANG storage system for the same fuel value was estimated in this analysis to cost approximately $10,000, to weigh ~1,100lbs, and require a tank of ~130gallon volume (6.5X space penalty). Therefore, even with the uncertainties in materials and processing inherent in a study of this nature, it is not likely that an ANG system would have significant probability of success in this market.

The search for a low-cost carbon fiber might make this monolithic material more reasonable in cost and a viable material for a variety of applications.

Metal-containing Activated Carbon Fibers - Introduction

The purpose of this task was to investigate and develop techniques to disperse metal nanoparticles in activated carbon fibers. The project is to determine the appropriate heating and activation conditions and to evaluate the catalytic and absorption properties of activated carbon fibers doped with metal.

Metal-containing activated carbon fibers offer several advantages. First, the isotropic pitch precursors are inexpensive and conventional melt spinning techniques can be used to produce fibers with diameters of from 10 to 15 microns, resulting in a high surface-to-volume ratio and facilitating mass transfer to and from the fiber. Also, because of the high surface-to-volume ratio, activation is extremely effective. As a result, the specific surface area of the activated carbon fibers is two to three times that of conventional activated carbon particles. Finally, the fibers can be inexpensively converted into a monolith form using slurry molding techniques.

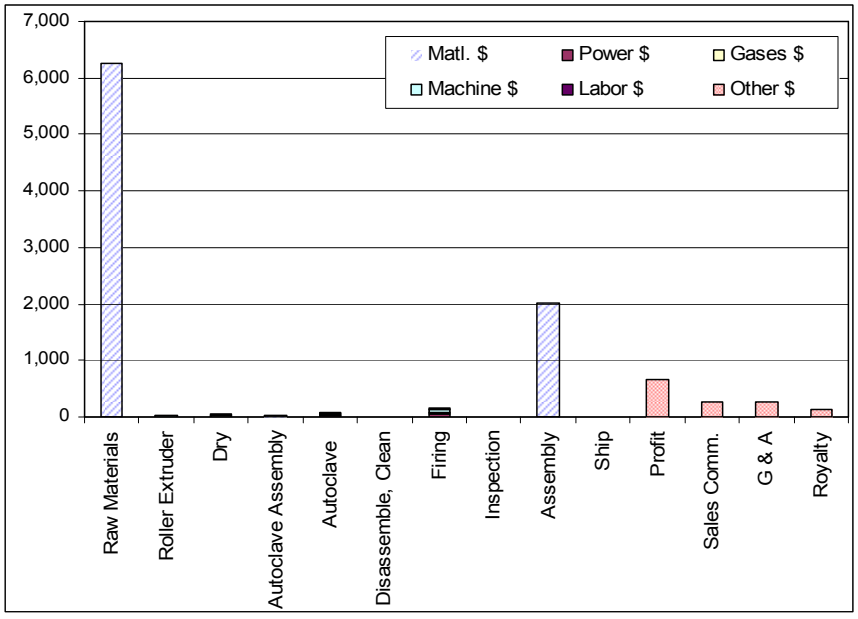

Figure 1. Cost / Price Factors for a 20 Gal. Gasoline Equivalent ANG Storage Device

Fiber Preparation

Figure 2 shows a flow diagram for the production of metal-containing activated carbon fibers. The process involves the mixing of a metal precursor (typically a metal salt) with an isotropic pitch. The mixture is then melt-spun into fibers using a bench-scale melt spinning apparatus. As-spun pitch-based fibers are stabilized in air in a conventional oven and carbonized at 1000°C in a helium atmosphere. Once stabilized and carbonized, the fibers are activated by exposing them to either CO_2 or steam and then heat-treated in a reducing or an inert atmosphere at elevated temperature. Activated, metal-containing carbon fibers are then characterized.

We have produced fibers from unmixed pitch (KU) and fibers containing silver (KAn), palladium (KPa), and mixtures of silver/palladium (KAP).

Fiber Characterization

The surface properties of the metal-containing activated carbon fibers were determined from nitrogen adsorption-desorption isotherms obtained at -196°C using a Micromeritics ASAP 2020 surface analyzer. All fibers were outgassed at 290°C overnight prior to each adsorption experiment. The Brunauer, Emmett, and Teller (BET) method was used to calculate the total surface area and pore volume. The Barrett-Joyner-Halenda (BJH) method was applied to the desorption branch of nitrogen adsorption-desorption isotherms to calculate the surface area and pore volume, the pore size distribution and average pore size (4V/S) in the meso-/macropore range. The micropore size distribution was calculated from the nitrogen adsorption-desorption isotherms measured at relative pressures ranging from 5×10^{-5} to 1 using Horvath-Kawazoe (H-K) method.

Figure 3 shows the pore size distribution for a selected set of activated carbon fibers. The pore size distribution curves for the Ag/Pd-containing activated carbon fibers exhibit a more pronounced peak at ~39 Å than that detected for the Pd-containing samples, even at their higher burnoff. An additional

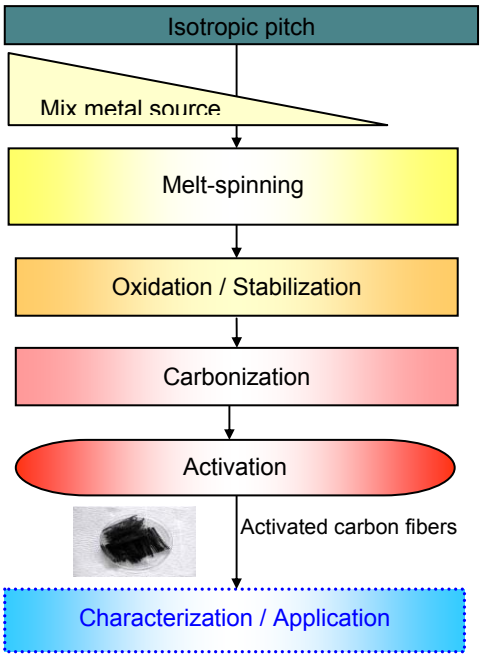

Figure 2. low process for the production of metal-containing activated carbon fibers.

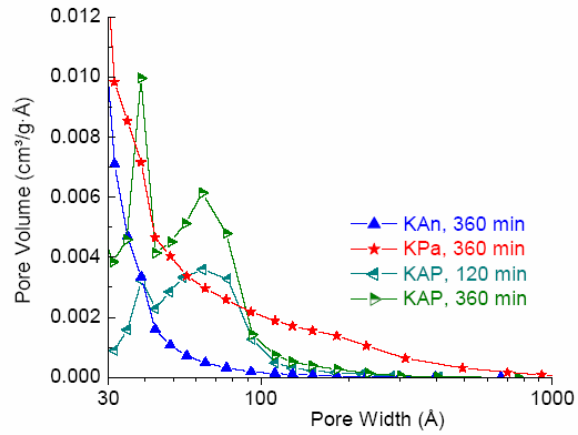

Figure 3. JH Desorption dV/dw pore volume plot of Ag-, Pd- and Ag/Pd-containing activated carbon fibers.

peak appears between 60 and 70 Å; this peak is not observed for the fibers containing the individual metals. Such peculiarities are most likely attributable to the formation of Ag/Pd alloy during the heat treatment, and they illustrate the synergistic effect of combining these two metals. These peculiarities of Ag-Pd pore structure formation may be useful for production of fibers with defined pore sizes.

Conclusions

We have successfully produced Pd- Ag- and Ag/Pd-containing activated carbon fibers. It was shown that the pore size distribution of these fibers is highly dependent on the type of metal contained in the fibers.

Additionally, the surface characteristics of the activated fibers will also be highly dependent on the type of metal present in the fibers.

Next steps will be the evaluation of these metal-containing carbon fibers for enhanced gas storage and for applications as catalyst. However, these applications are outside the scope of this program and will not be pursued here.